

TABLE 2. Stars counts in each branch of the CMD.

Branch	Expected	Found
MS	114-122	112
SGB	16-26	17
RGB	4-9	10
HB	0.6-1.2	0(?)

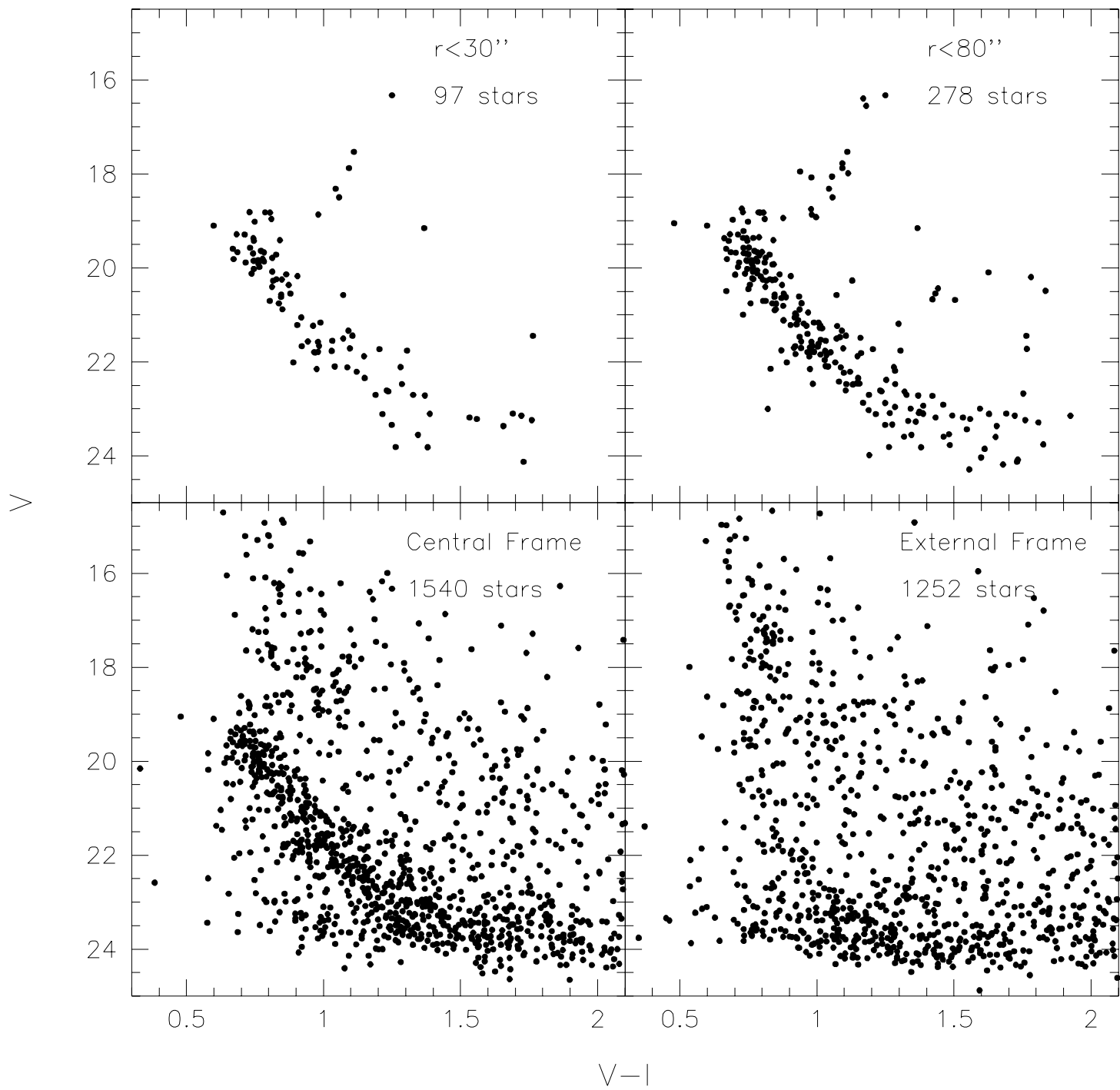


TABLE 3. Star counts and LF of Pal 1.

V	$r < 30''$ (0.791) ^a		$30'' < r < 270''$ (59.94) ^a		$r > 350'$ (108.0) ^a		Compl. cen./ext.
	stars	ψ^b	stars	ψ^b	stars	ψ^b	
16.88	12.00	0.0510	48.00	0.0006	69.00	0.0022	1.00/1.00
19.75	32.00	0.6693	61.00	0.0119	33.00	0.0051	1.00/1.00
20.75	20.00	0.4162	78.00	0.0164	34.00	0.0052	1.00/1.00
21.75	27.00	0.5594	110.00	0.0210	62.00	0.0096	1.00/1.00
22.75	16.80	0.3120	201.83	0.0141	272.35	0.0420	0.95/0.89

^aarea covered in arcmin²^b ψ =stars/mag/arcmin².

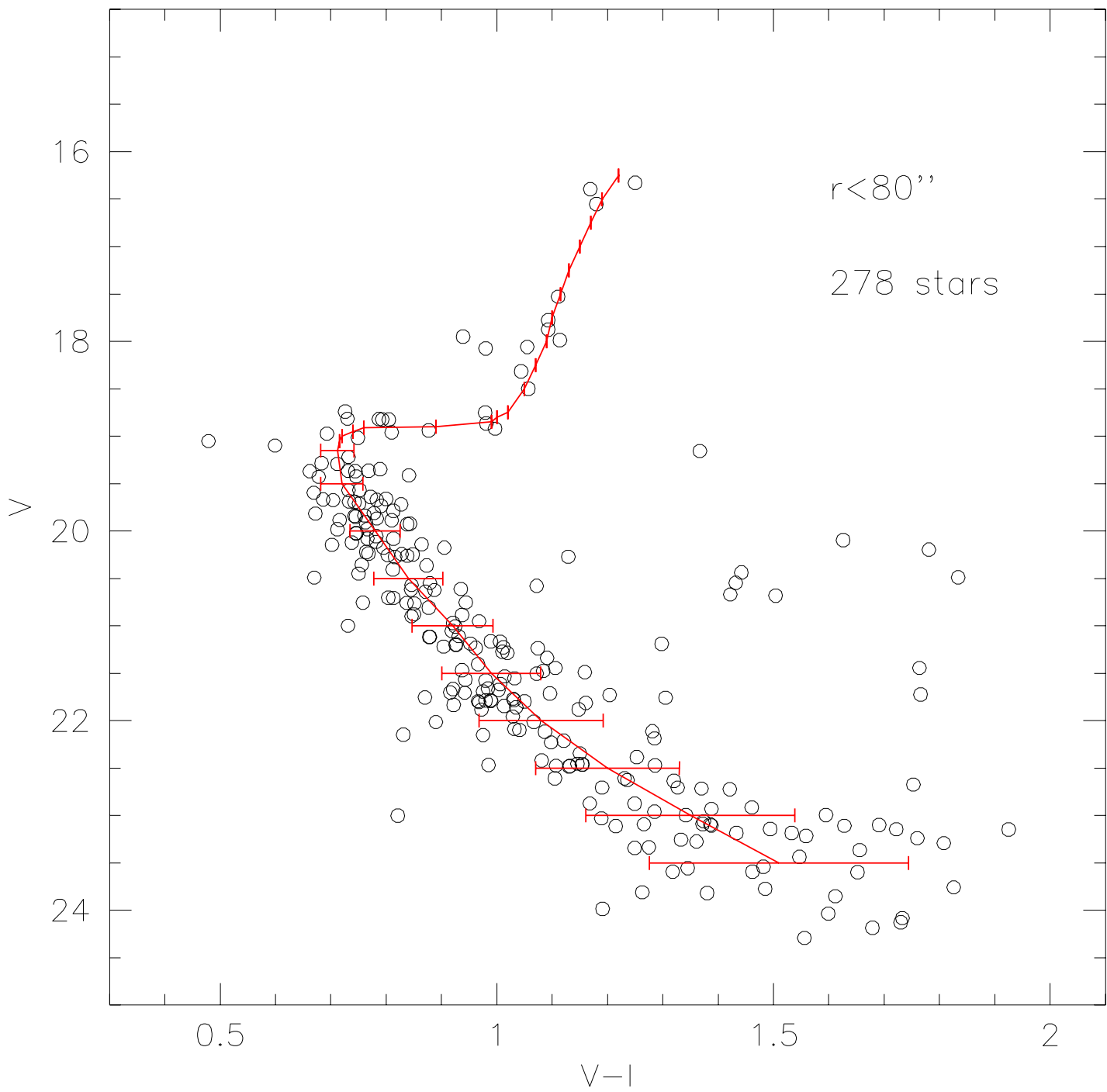
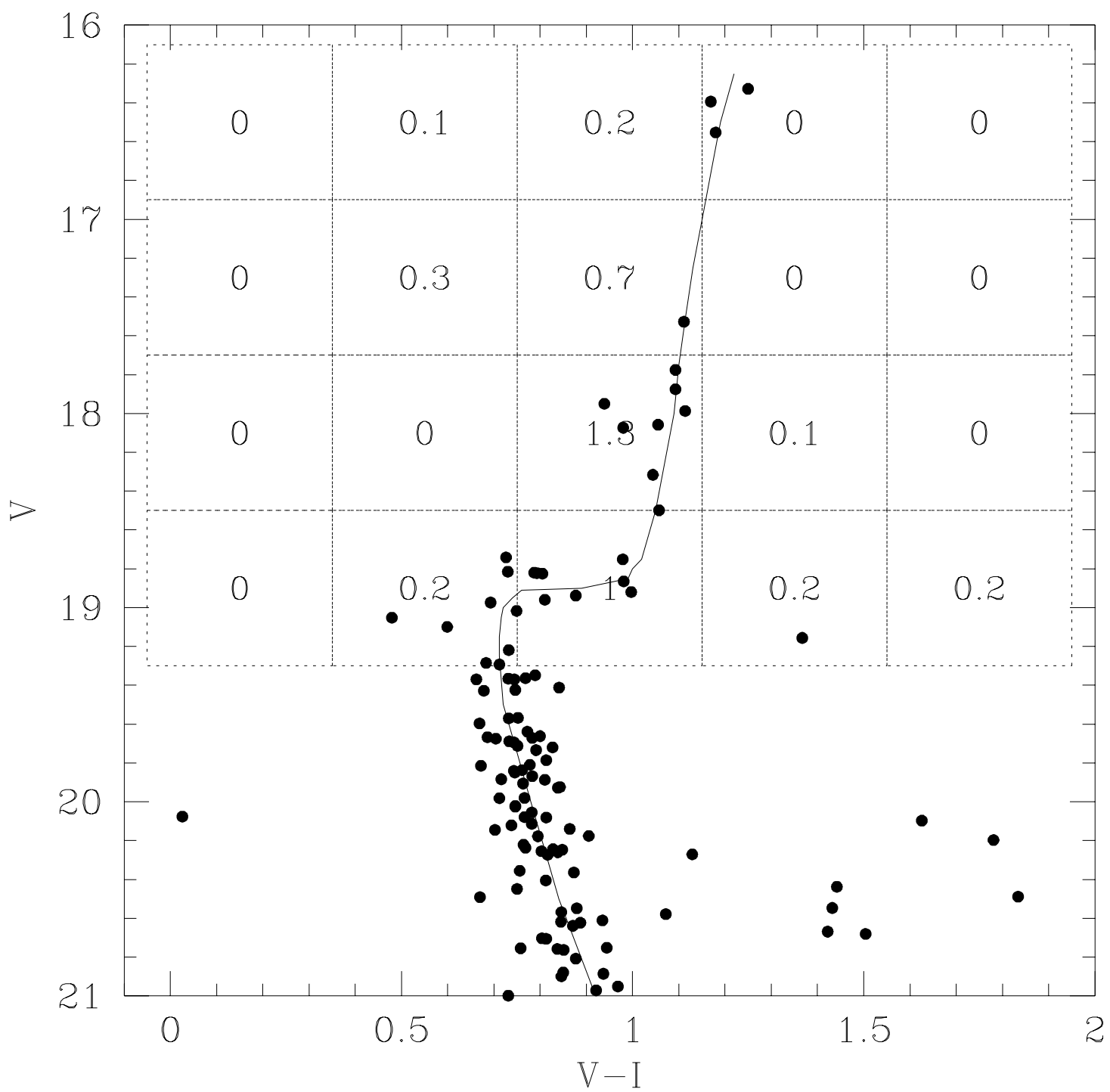
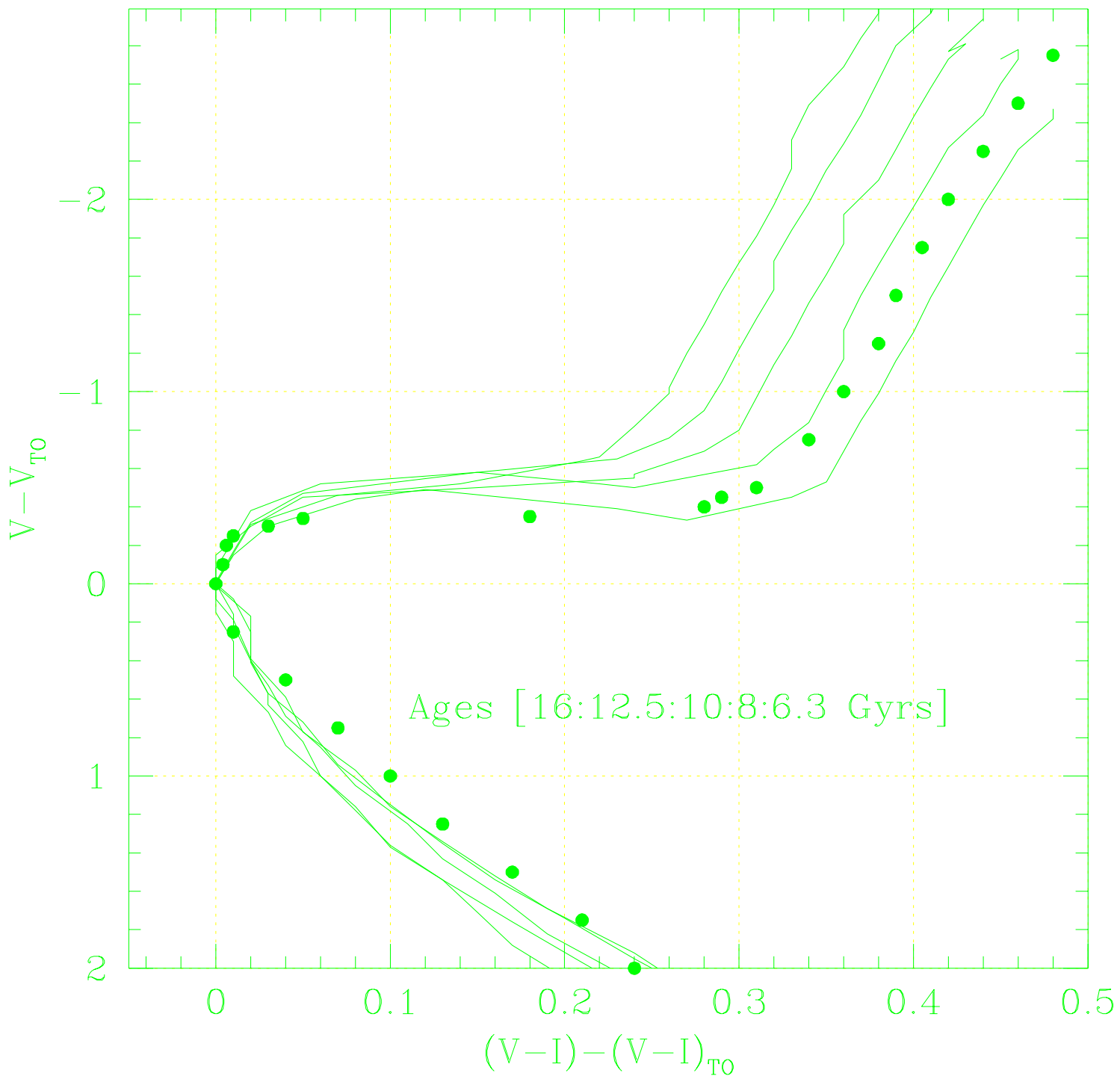
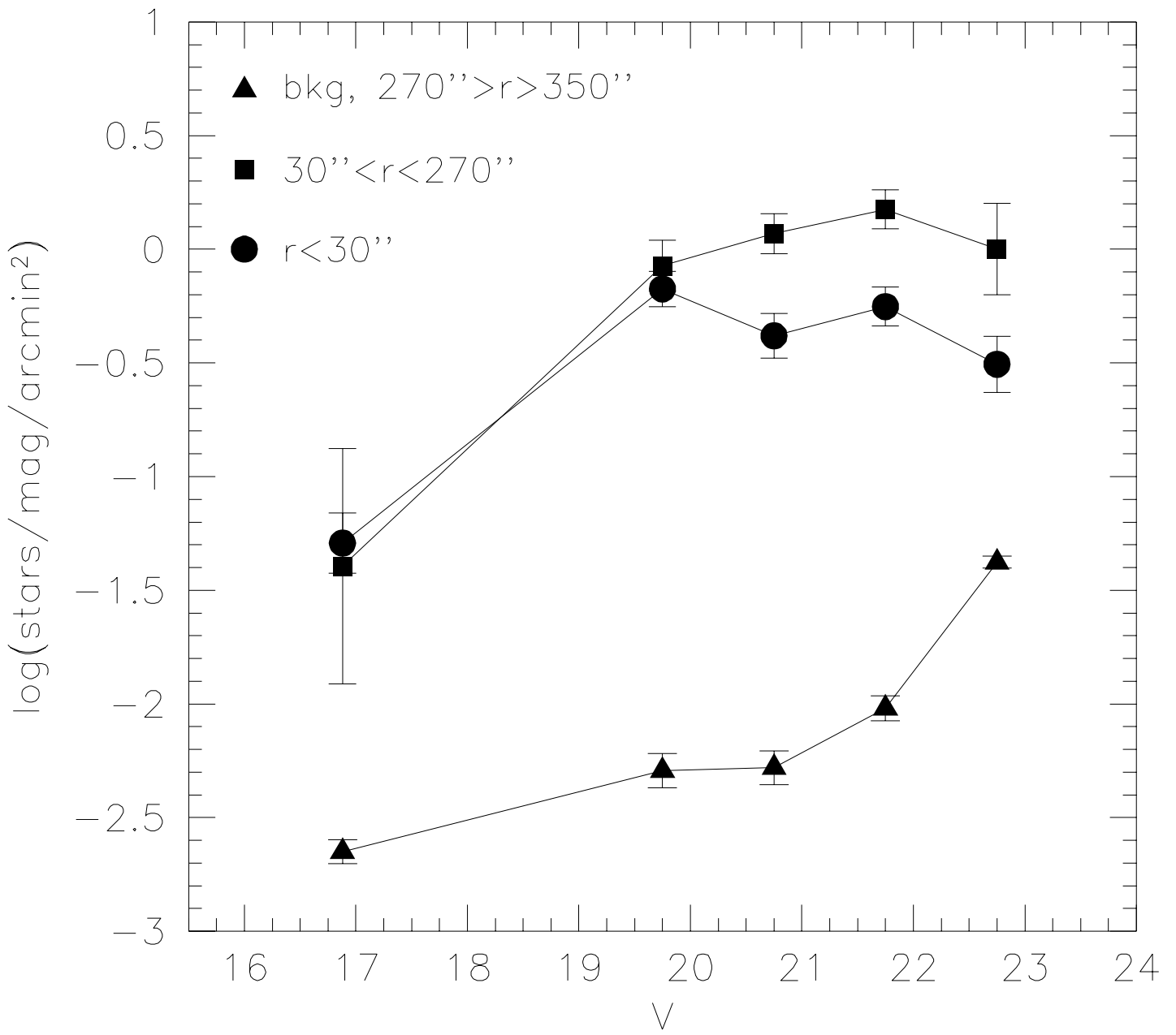


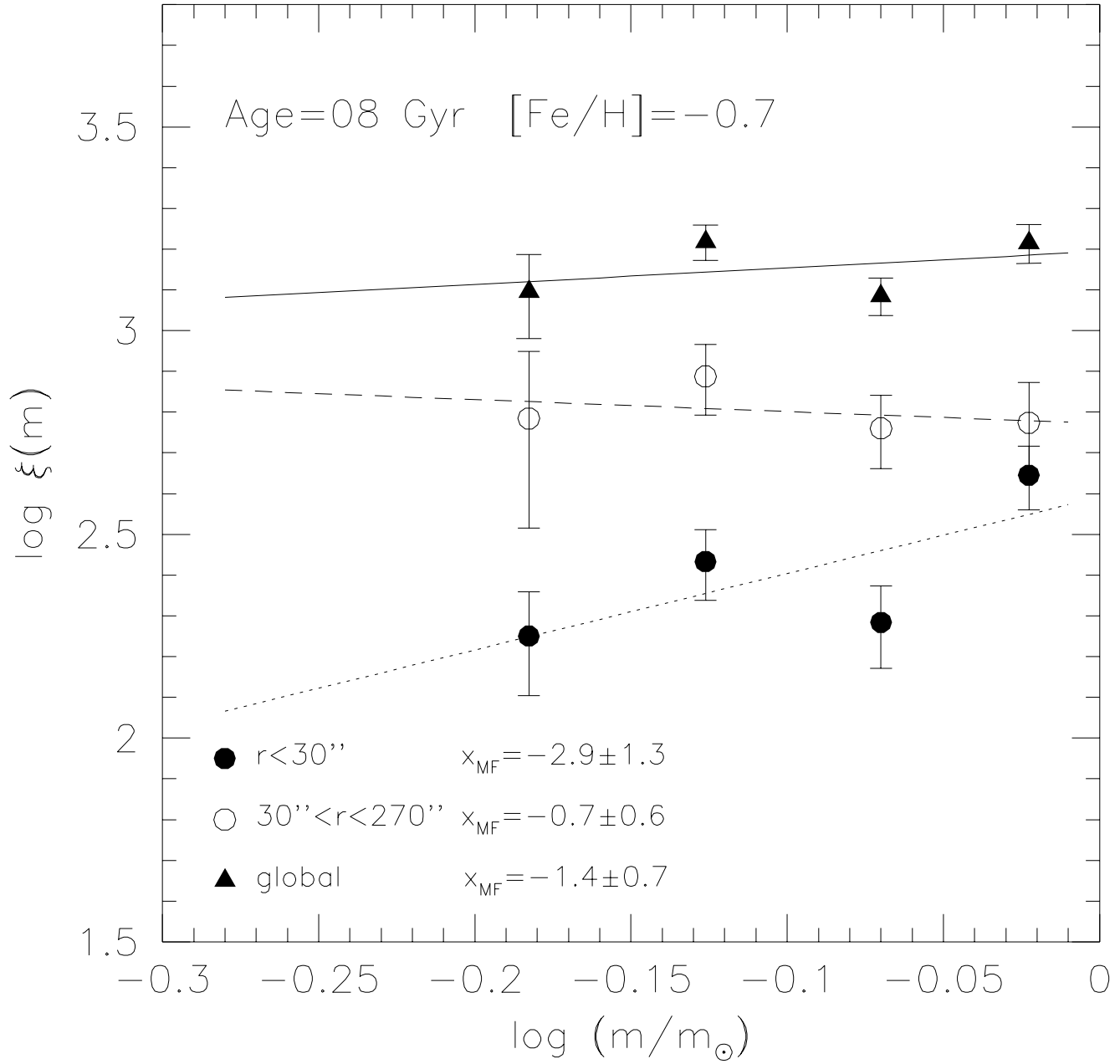
TABLE 4. Global parameters of Palomar 1.

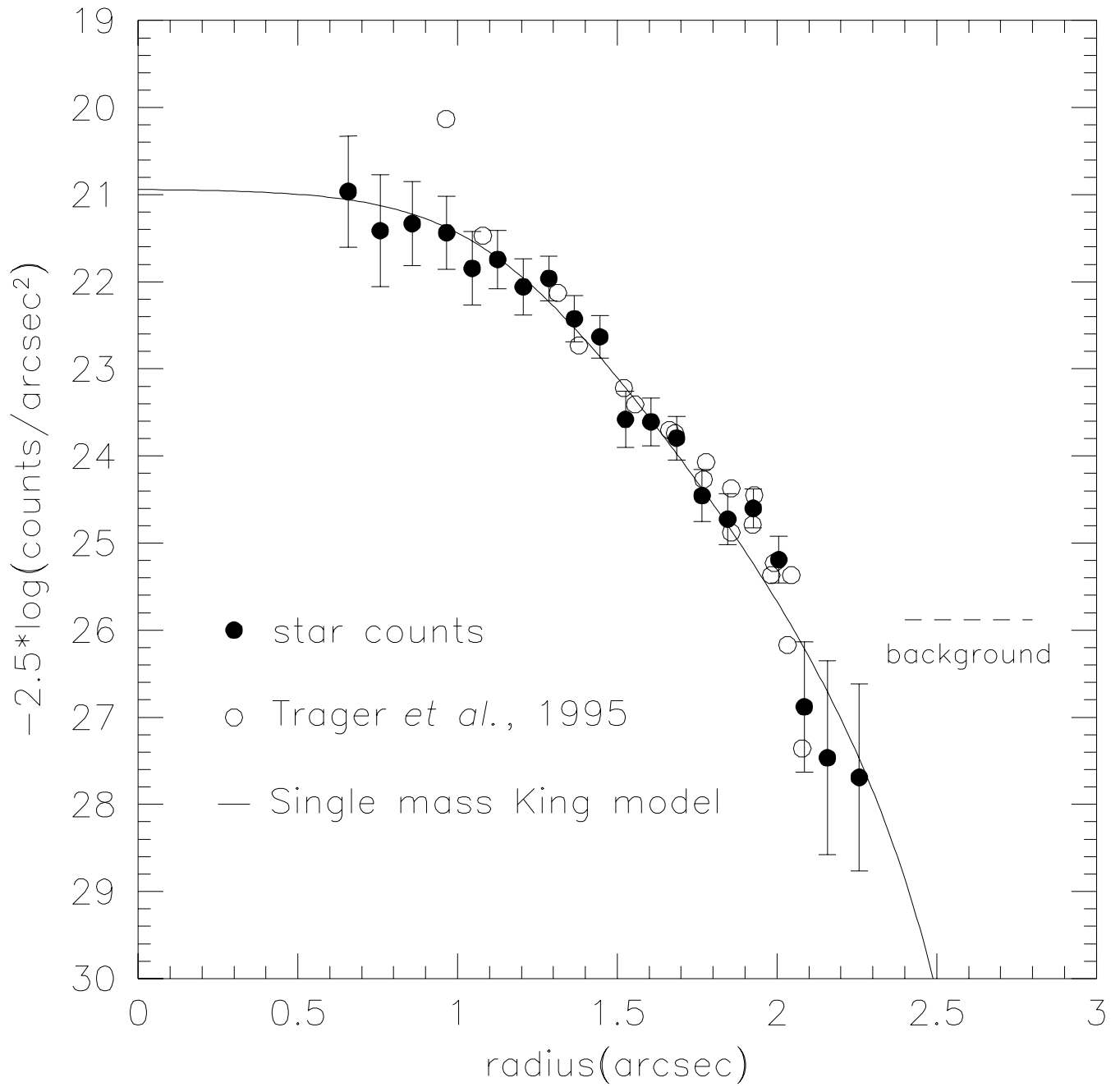
Parameters	Value
V_{TO} :	19.25 ± 0.20
$(V-I)_{TO}$:	0.71 ± 0.03
$[Fe/H]$:	-0.60 ± 0.20
age [Gyr]:	$8.0 \div 6.3$
$(m-M)_0$:	15.25 ± 0.25
$E(V-I)$:	0.20 ± 0.04
$E(B-V)$:	0.15 ± 0.03
R_{\odot} [kpc]:	11.2 ± 1.3
R_{GC} [kpc]:	17.3 ± 1.6
Z_{GP} [kpc]:	3.7 ± 0.4
x_{MF} :	-1.4 ± 0.7
c :	1.60
r_c :	$13.5''$
r_h :	$41''$
r_t :	$525''$
$\mu_V(0)$:	20.93 ± 0.25
$\mu_V(r_h)$:	23.52 ± 0.25
M_V :	-2.54 ± 0.50
n_{tot} :	342 ± 21
$\log(m/m_{\odot})$:	3.1 ± 0.3

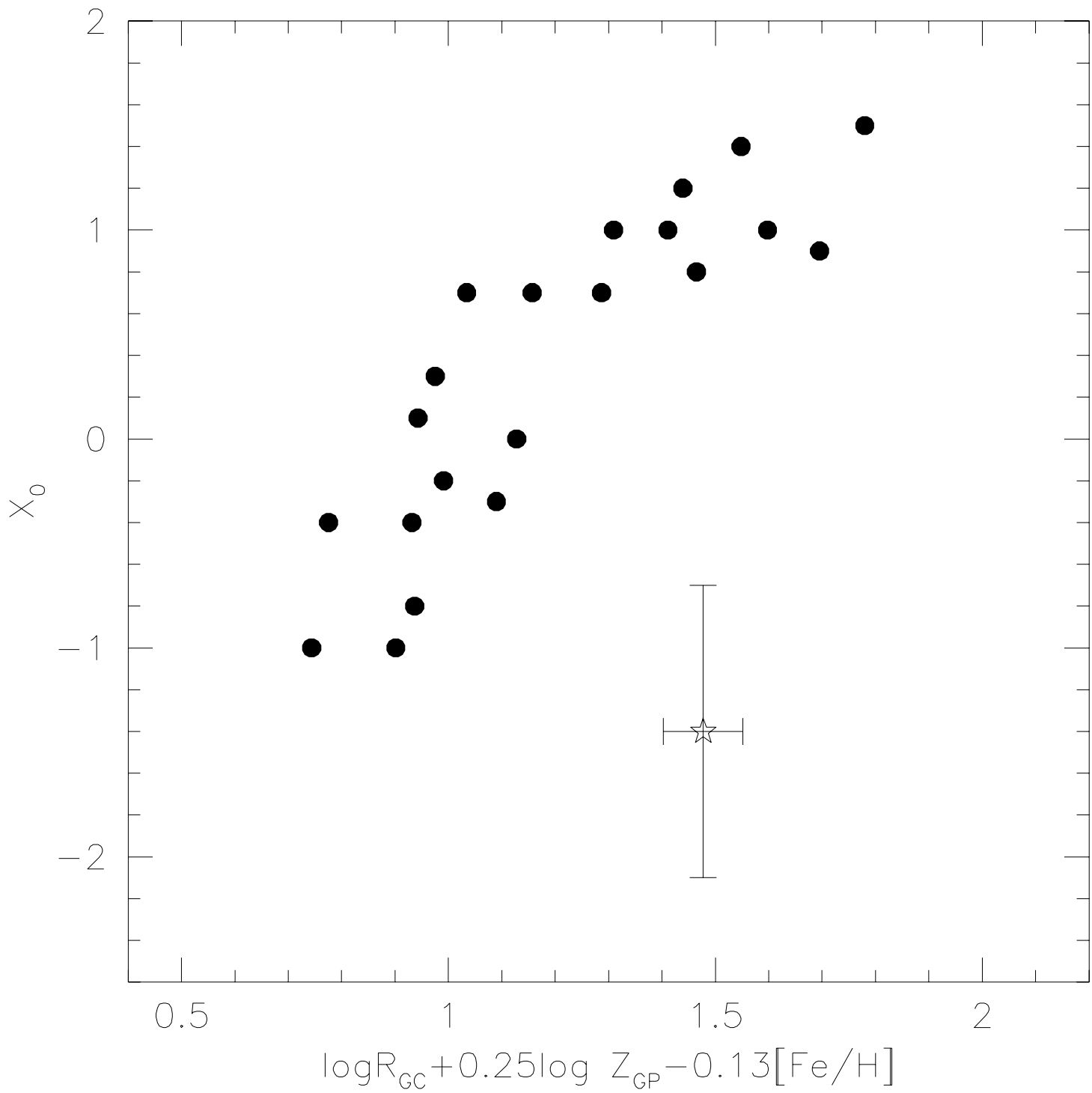












Pal 1: Another young Galactic halo globular cluster? ¹

A. Rosenberg

Telescopio Nazionale Galileo, Osservatorio Astronomico di Padova, Italy

I. Saviane, G. Piotto

Dipartimento di Astronomia, Università di Padova, Italy

A. Aparicio

Instituto de Astrofísica de Canarias, Spain

S. R. Zaggia

Osservatorio Astronomico di Capodimonte, Italy

Received _____; accepted _____

¹Based on observations made with the Isaac Newton Telescope operated on the island of La Palma by the Isaac Newton Group in the Spanish Observatorio del Roque de los Muchachos of the Instituto de Astrofísica de Canarias.

ABSTRACT

Deep V and I CCD images of the loosely populated Galactic globular cluster Pal 1 and the surrounding field have been obtained with the Isaac Newton Telescope. A color magnitude diagram down to $V_{lim} \sim 24$, and a luminosity function complete down to $V_{lim} = 23.25$ have been constructed.

Adopting a reddening $E(V-I) = 0.20 \pm 0.04$ and comparing the CMD of Pal 1 with 47 Tucanae, we obtain a distance modulus $(m - M)_0 = 15.25 \pm 0.25$, indicating that Pal 1 is located 3.7 ± 0.4 kpc above the Galactic disc and 17.3 ± 1.6 kpc from the Galactic center.

Comparison with 47 Tuc and M71 shows that Pal 1 must be significantly younger. The best fitting isochrones (Bertelli et al, 1994) give an age between 6.3 and 8 Gyrs, which would make Pal 1 the youngest Galactic globular cluster so far identified, casting some doubt on the real nature of this object.

The luminosity function shows some evidence for mass segregation, consistent with the very short relaxation time. The global mass function can be fitted with a power law of slope $x = -1.4 \pm 0.7$. This mass function is anomalously flat, suggesting either a strong dynamical evolution or an initial mass function significantly different from most of the other halo globular clusters.

A discussion on the possible nature of Pal 1 is presented.

Subject headings: Globular clusters: individual: (Palomar 1)

1. Introduction

The globular cluster (GC) Pal 1=C0325+794 ($\alpha_{2000} = 3^h 33^m 4$, $\delta_{2000} = +79^\circ 35'$; $l = 130^\circ 1$, $b = 19^\circ 0$) is a very faint star cluster ($M_V = -2.54$; Webbink 1985, W85) discovered by Abell (1955) on the Palomar Sky Survey plates. From its position in the Galactic halo at about 14 kpc from the Sun, 19 kpc from the Galactic center, and 4.5 kpc above the Galactic plane (W85), Pal 1 has been classified as a GC.

It was searched for variable stars by Kinman & Rosino (1962, KR62). They counted 100 stars, mostly between $V=20$ and $V=22$, but no variables were found. KR62 also remark that, since many galaxies are seen in the field, the absorption cannot be high.

Previous studies of the color magnitude diagram (CMD) include Ortolani & Rosino (1985, OR85) and Borissova & Spassova (1995, BS95). OR85 noted that:

(1) The CMD of Pal 1 is peculiar for a GC. The turn-off (TO) is well defined but the red giant branch (RGB) is very poor, truncated at $V \sim 16.3$, and the horizontal branch (HB) is absent;

(2) There is some resemblance with other GCs such as Pal 13, Pal 12, or E3. However, OR85 also suggest that “some resemblance to an old open cluster must be noted, mostly for the anomalous inclination of the sub giant branch (SGB)”.

BS95, reported CCD photometry in the Thuan-Gunn system of a field of 7×4.7 arcmin² centered on the core of the cluster, reaching a limiting magnitude of $g = 21.5$. They also estimate an age in the interval 12-14 Gyr, which would make Pal 1 a typical GC.

The first determination of the metallicity was made by W85, from the correlation between the dereddened subgiant colors and the high-dispersion spectroscopic metallicities, obtaining $[\text{Fe}/\text{H}] = -1.01$, adopting $(B-V)_{0,g} = 1.08$ and $E(B-V) = 0.15$ from an unpublished paper by Da Costa (1984). The error on the estimate of the $(B-V)_{0,g}$ is unknown (cf. Section 4) making this result very uncertain. BS95 give $[\text{Fe}/\text{H}] = -0.79$ (No error is quoted).

With respect to the reddening, W85 gives $E(B-V)=0.15$ (based on the neutral hydrogen column density plus galaxy counts), OR85 estimate $E(B-V)=0.1$ from the Galactic position, and BS95 give $E(g-r) = 0.16$ (from comparison with the theoretical isochrones by Bell & Vandenberg 1987). The estimated distance modulus ranges between 15.68 (W85) and 15.38 ± 0.15 (BS95). BS95 derived an age of 12–14 Gyrs with a nominal uncertainty of 2 Gyrs.

The results from these works are rather uncertain, due to the small number of cluster stars and the contamination by Galactic foreground and/or background objects.

Here we present a new, extensive study of Pal 1, based on a set of images collected at the INT 2.5m Telescope covering the entire cluster (Figure 1), and a field at 10 arcmin from the center, taken for the purpose of studying the non-cluster star contamination. The observations and data reductions are presented in Section 2. The color magnitude diagram is discussed in Section 3. In Section 4 we will address in more detail the problem of the real nature of this cluster, trying to establish its distance and age. We also present the luminosity (LF) and mass (MF) functions (Section 5), and the structural parameters of the cluster (Section 6).

2. Observations and reductions

The observational data base consists of 17 frames, 9 in the V band (with a total integration time of 7260 s), and 8 in the I band (with a total integration time of 3230 s) centered on the cluster. We also collected 6 V (total exposure of 6060 s) and 6 I (2490 s) frames of an external field located 10' West from the cluster center with a suitable overlap ($\simeq 1'$) with the central frame for the internal comparison of the photometry of the two fields (see Table 1 for a detailed log of the observations).

The data was obtained at the INT 2.5m telescope on November 8, 9 and 10, 1994, at the Observatory of Roque de los Muchachos in La Palma, Canary Islands, Spain. The CCD used was an EEV 1242×1152 . The CCD scale is $0''.54$ per pixel, and the resulting field of view is 11.2×10.3 arcmin².

The pre-processing of the images was done in a standard way, briefly summarized below. First the constancy of the bias level across the image was checked by taking several bias images on each night: no gradients were detected, and we verified that the bias level was fully consistent with the value in the overscan area of the scientific frames. This constant value was therefore subtracted from each image. As a second step, each image was corrected for the varying sensitivity across the CCD frames. About seven sky flat-fields were taken per night in both filters, and the raw images were divided by the resulting median flats, using the appropriate reference flat according to the night and filter.

The seeing conditions were almost constant during the three nights, so long exposure images were averaged to obtain reference frames for each field/filter: for the central field, we used the 8 V and 7 I long exposures, while for the external field the 5 V and 4 I long exposures were used. The photometry of the master frames was obtained using DAOPHOT II (Stetson 1987).

Calibration of the raw photometry was accomplished in three stages. First, both the standard star magnitudes and the object frame magnitudes were referred to a common instrumental system, ensuring that the same fraction of the stellar flux had been sampled in both cases. We assumed that, when a suitably large aperture is chosen, the different percentages of the flux which are left out add negligible corrections to the magnitudes of the standard and object stars: all magnitudes were corrected to this common aperture. The radius was fixed using the standard stars observed in the worst seeing conditions. We established the limit at which the wings of the PSF merged into the background, and

set the fixed aperture $\sim 1''$ larger than this limit (i.e. $6''.5$). For the standard stars, this large aperture was used, while for the Pal 1 stars aperture corrections were calculated. Actually, for the cluster frames we have PSF magnitudes, though the instrumental PSF magnitudes (m_{PSF}) and the aperture magnitudes (m_{AP}) have the same zero point (Stetson 1987; see also Aparicio & Gallart 1995). The aperture corrections were calculated using the standard stars. We followed the same method used by Aparicio & Gallart (1995). This method is based on the fact that the aperture corrections are a function of the seeing alone. Figure 2 shows the dependence of the aperture correction on the full-width at half-maximum (FWHM) of the stellar images. The internal dispersion (standard deviation) is of 0.02 mag. As a second step, the dependence on the airmass and the exposure time was removed. According to the La Palma User Manual, the shutter delay time is of ~ 4 milliseconds. As the exposure times on the standard stars are between 3 and 10 sec, we expect an error < 0.001 magnitudes due to the shutter.

The conversion from instrumental to standard magnitudes was based on a total of 102 measurements from multiple exposures of 23 standard stars from the list of Landolt (1992). Independent calibrations for each night were made. As the coefficients of the calibration curves were the same within the errors, we adopted their mean value. Also the atmospheric extinction coefficients were independently determined for each night. Because of the stability of the atmospheric conditions, we decided to adopt mean values. The (V-I) colors of the standards range from -0.53 to 1.95 mag, and the V magnitudes from 12.2 to 16.1 mag. The transformation from the instrumental magnitudes to the Landolt (1992) magnitude system was:

$$V - v = 24.95 + 0.05(V - I), (\sigma = 0.02)$$

$$I - i = 24.01 - 0.02(V - I), (\sigma = 0.03)$$

where V and I are the standard magnitudes, and v and i the previously defined normalized

magnitudes.

Stars brighter than $V=16.0$ were saturated in the long exposure images. Their magnitudes were measured on the short exposure images. After the calibration to the standard photometric system, we checked the zero points of the magnitudes from the short exposure images ($V \leq 16.0$) and the long exposure images ($V > 16.0$): the mean difference is of 0.002 magnitudes in V and 0.004 magnitudes in I .

3. The color–magnitude diagram

The CMDs for the inner $30''$ and $80''$ from the center of the cluster, and for the whole central and external frames are shown in Figure 3.

The main features of the CMD can be clearly identified in the two central regions, though some contamination by foreground objects is present. The CMD of the inner $80''$ is better shown in Figure 4, where the adopted fiducial points and main sequence (MS) widths (1 sigma) are also plotted. The fiducial points have been obtained assuming that the color distribution is Gaussian and determining the mean color and sigma in each 0.5 V magnitude interval and using a k -sigma clipping algorithm ($k=2.5$). The fiducial points above the TO have been obtained simply drawing a line through the data. From the CMD in Figure 4 and from the fiducial points, we estimate that the TO of Pal 1 is located at $V_{TO} = 19.25 \pm 0.20$ and $(V - I)_{TO} = 0.71 \pm 0.03$.

Given the high field contamination, one could question if the adopted interpolation realistically represents the cluster giant branch for $V < V_{TO}$. To test this point, we calculated the expected number of field stars, scaling for the sampled area, on the basis of the background field CMD: in a circle of $80''$ radius, for $V < 19.25$, 4.3 field stars are expected, while in the CMD of Figure 5 there are 28 stars. This means that at least 80 %

of the stars from V_{TO} to $V \sim 16$ are likely to be real cluster members. We calculated also the expected number of field stars in square boxes of arbitrary size within the CMD, again after scaling for the sampled area: the result is sketched in Figure 5, where the stars in the inner $80''$ are plotted and the numbers represent the field stars expected in each box. It is quite evident that most of the “evolved” stars in Figure 4 and Figure 5 are probably cluster members.

The relative number of stars in different regions of the CMD may also be estimated from stellar evolution theory. Using the isochrones by Bertelli et al, (1994, B94) and assuming a Salpeter MF (the result does not change significantly adopting a different MF slope), we can calculate the number of stars which are expected in each phase of the CMD for different metallicities and ages. As reported in Table 2, the counts within $80''$ from the center are consistent with the expected ones, which have been calculated assuming ages from 6.3 to 20 Gyrs and metallicities from -0.3 to -1.0 . The star counts have been normalized to the total number of stars. Furthermore, four RGB stars of Pal 1 have been studied spectroscopically (Rosenberg et al, 1997), and their radial velocities are compatible with membership in the cluster.

One could ask if any of the 8 stars in the box of the CMD defined by $0.65 < (V-I) < 0.85$ and $18.75 < V < 19.25$ are binaries. Unfortunately, the broadening of the MS due to the photometric errors and the small statistical sample does not allow us to draw any conclusions about the presence of a binary sequence. The presence of binaries around the TO could affect the magnitude (but not significantly the color) of the TO itself and the discussion of the cluster age. We can make an estimate of the possible error in the age by assuming that 50 per cent of the stars are binary objects. In this case, the true TO luminosity would be ~ 0.35 mag fainter. Since the age will be estimated from the color difference between the TO and the RGB (cf. Sect. 4), a change in color of the RGB

reference point due to the change in the TO location, would be 0.03 mag towards the blue. This would increase our measured age by $\simeq 2$ Gyrs. On the other side, making the TO 0.35 mag fainter, would increase the age by at most ~ 3 Gyr (from eq. 5b in Buonanno, Corsi, & Fusi Pecci 1989).

A final comment on the possible presence of HB stars. In their preliminary work, OR85 could not find any star in this phase, while BS95 suggest that 5 stars located $\simeq 3.2$ mag above the TO in their CMD could be HB stars. Statistically ~ 1 star is expected to be in this phase according to the evolutionary tracks, so we can not exclude the possibility that one or two stars at $V_{\text{HB}} \sim 16.3$ in Figure 4 are part of the red clump of the cluster’s HB. It is impossible to say anything on the presence of a HB in the complete CMD of Figure 3.

From this discussion, it must be clear that any cluster parameter in the literature (and in the following) derived from the location of the HB, must be considered only tentative and uncertain.

4. Determination of the main parameters

Since a precise value of the metallicity is crucial for the age determination, we have carried out spectroscopic observations in order to determine this parameter following the method of Armandroff & Da Costa (1986,1991). The detailed analysis of our data set, which is given in Rosenberg et al, (1997), yields a value $[\text{Fe}/\text{H}] = -0.60 \pm 0.20$ dex, and we will adopt this metallicity in the following.

As already discussed in the introduction, all the previous determinations of the reddening established a value around $E(\text{B}-\text{V}) = 0.15$; in order to have an independent estimate of this quantity, we inspected the Burstein & Heiles (1982) maps, which give an $E(\text{B}-\text{V})$ between 0.12 and 0.15. In the present paper, we will assume $E(\text{B}-\text{V}) = 0.15 \pm 0.03$,

which implies $E(V-I) = 0.20 \pm 0.04$ (adopting $E(V-I) = 1.28 E(B-V)$, Dean et al, 1978).

With the adopted values for the reddening and metallicity, it is now possible to determine the distance modulus of Pal 1 by comparison with other clusters of similar metallicity, after establishing a reliable set of parameters for the reference clusters.

In this respect, 47 Tuc [Alcaino & Liller 1987, (AL87), Grundahl 1996 (G96), Kaluzny et al, 1997 (K97)] and M 71 [Richer & Fahlman (1988,RF88), Hodder et al (1992,H92), Grundahl 1996 (G96)] are the only GCs that can be used for this comparison. Their metallicity is around $[Fe/H] = -0.7$ and they have accurate published VI photometry from the RGB to several magnitudes below the TO (Note that the diagram by G96 is the only CMD available in V vs. $(V-I)$ for M71). A careful discussion of the 47 Tuc parameters can be found in Hesser et al, (1987, H87), and we will assume their values for the cluster reddening, metallicity and distance: $E(B-V) = 0.04 \pm 0.01$ [corresponding to $E(V-I) = 0.05$], $[Fe/H] = -0.8$ and $(m - M)_V = 13.35 \pm 0.2$. The quoted distance modulus is a mean of the two values found by H87, namely $(m - M)_V = 13.4$ and 13.3 from a comparison with the theoretical ZAHB and the field subdwarfs, respectively. In the following, we will refer to 47 Tuc as reference cluster.

We plotted the three available CMDs of 47 Tuc together, and evaluated the zero-point differences in the turnoff region. There are overall differences of less than 0.02 mag in color, with the K97 sequences in between the other two. Given the high statistical significance (more than 15,500 stars) and the depth (~ 3.5 mag below the TO) of the K97 sample, we chose this dataset as the 47 Tuc template.

Figure 6 displays the absolute fiducial sequences of 47 Tuc (open triangles) and, M71 (open circles). After a shift of $\Delta(V - I) = 0.24$ and $\Delta(m - M)_V = 0.38$ the fiducial line of M71 perfectly overlaps 47 Tuc. The sequence of 47 Tuc has been used to determine the distance modulus of Pal 1. After correcting the CMD of Pal 1 for the adopted reddening,

the apparent distance modulus has been computed by fitting its lower MS to that of 47 Tuc. The fit was carried out in the absolute magnitude interval $5 < M_V < 7$, where evolutionary effects due to possible differences in age should be minimal.

Allowing $E(V-I)$ to vary from 0.16 to 0.24, the apparent distance modulus of Pal 1 varies in the interval $15.51 < (m - M)_V < 15.94$, as shown in Figure 6. Taking into account the uncertainty in the calibration, in the adopted reddening, in the fit, and in the distance of the comparison clusters, the absolute distance modulus is $(m - M)_0 = 15.25 \pm 0.25$.

As shown in Figure 6, a good match of the Pal 1 giant branch would be obtained for a value of the reddening $E(V-I) \simeq 0.18$. On the other hand, the position of the RGB is controlled not only by a cluster metallicity, but also by its age, and, as we will see later in this section, Pal 1 seems to be younger by at least 6 Gyr than normal GCs. Therefore, we expect that the stars which are evolving along the RGB of this cluster are more massive (and hence hotter) than those of the comparison clusters (which have a ‘normal’ age, cf. H87 and G96).

In this case, the reddening must be higher than the value obtained from a direct comparison with the sequences of 47Tuc and M71, since its bluer RGB requires a smaller shift in order to be superposed on the reference RGB. In order to estimate this effect, we analyzed a set of isochrones from Bertelli et al, for $[Fe/H] = -0.7$, and found a relative shift of $0.03 \div 0.04$ mag between the RGBs for the expected age interval. A value $E(V-I) \simeq 0.21 - 0.22$ is therefore a better estimate of the cluster reddening. This is almost coincident with the adopted value.

The most striking feature of the Pal 1 CMD which emerges from the comparison with M 71 & 47 Tuc is the larger color difference between the TO and the RGB base: it is well-established (see e.g. Vandenberg, Bolte & Stetson 1990) that the color width between the TO and the RGB is a function of the cluster age and metallicity. Since the template

clusters and Pal 1 have similar metallicities, the discrepancy which is observed for Pal 1 is most likely due to a younger age.

This result is confirmed by a direct comparison of the Pal 1 CMD with a set of theoretical isochrones taken from the library of B94. In order to put a constraint on the subset of model ages to be used, we first compare in Figure 7 the CMD of Pal 1 with the models, registering both of them to the TO. In this way, the color width between the TO and the RGB base can be used to select a subsample of isochrones. The figure clearly shows that a standard 16 Gyr isochrone is not able to reproduce the morphology of the diagram, and we have to assume an age between 6.3 to 8 Gyrs in order to fit the cluster’s fiducial points. This would make Pal 1’s age of the order of the oldest open clusters.

This result is furtherly confirmed by Figure 8 which shows that the 8 Gyr isochrone is the one that better reproduces the overall morphology of the CMD in the $(V - I)_0, M_V$ plane when we adopt the distance modulus and reddening previously discussed. A slight blueward offset of 0.03 mag was applied to the isochrones in order to superpose the main sequences and giant branches: this offset is entirely within the uncertainties in the value of the reddening.

If we adopt the TO magnitude and the (very uncertain) HB magnitude discussed in Section 3, we would have a $\Delta V_{TO}^{HB} = 2.95$, corresponding to an age of 8.3 Gyr (Buonanno et al, 1989, eq. 5b).

In summary, from the comparison with the theoretical isochrones and the old GCs we can conclude that Pal 1 must have an age significantly lower than the bulk of the Galactic GCs.

The adopted distance modulus corresponds to a distance from the Sun of 11.2 ± 1.3 kpc, a distance from the Galactic center $R_{GC} = 17.3 \pm 1.6$ kpc and a height $Z_{GP} = 3.7 \pm 0.4$

above the Galactic plane (we adopted a distance Sun–Galactic Center $R = 8.0 \pm 0.5$ kpc, Reid 1993)

In view of its position in the Galaxy, it is not very likely that Pal 1 is an old open cluster, though this possibility can not be ruled out. We note that in the compilation by Friel (1995, F95) of the oldest open clusters, none of them has $Z_{\text{GP}} > 2.4$ kpc. On the other hand, the metallicity, though very low for an open cluster, would still be consistent with the radial abundance gradient for the old open clusters proposed by F95. As discussed in Section 6, Pal 1 seems to be more concentrated than normal old open clusters, while its concentration parameter $c = 1.6$ is typical for a globular cluster (Trager, King & Djorgovski 1995).

5. Luminosity and Mass functions

We have obtained the stellar luminosity functions for two radial regions of Pal 1: inner, $r \leq 30''$, and outer, $30'' < r < 270''$. We extracted the LFs using only stars falling within 3 sigmas of the fiducial line of the MS. In order to facilitate the star counts, we linearized the MS by subtracting from each star the V–I color corresponding to the V magnitude along the MS. We obtained the LFs in one magnitude bins, with the exception of the first bin which includes all the evolved stars. The two LFs are reproduced in Figure 9, together with the LF of the background obtained in the same way. The outer LF of Pal 1 has been arbitrarily shifted in order to match the first two bins of the inner LF.

Each LF was corrected for completeness. We used an approach similar to that described in Piotto et al (1990). The completeness was estimated in the magnitude range $V=19.5-25.0$ by adding artificial stars to the original frames in 0.25 magnitude intervals, and checking what percentage was recovered in each region, after a reduction stage equal

to that of the original images. The artificial stars were added to the average frames. The I magnitudes for the stars were set using the (V–I) color of the MS. We considered as recovered stars only those identified both in the V and I frames. For the central field we reach the 50% completeness at $V \simeq 23.7$, and $V \simeq 23.5$ for the external one. When doing star counts we stopped at $V = 23.25$, well above the 50% limit (see Table 3).

The LFs were also corrected for field star contamination by subtracting the star counts coming from the external frame ($r > 350''$, see Figure 9) to the counts of the central frame, after correcting for completeness and area coverage.

The completeness corrected star counts (Columns 2,4, and 6) and the luminosity function (Columns 3,5,and 7) for each radial bin are reported in Table 3, where in the last column we present also the values of the completeness correction adopted for the central and the external field.

The error bars of the LFs include the Poisson errors of both the cluster and background counts, plus the uncertainty in the completeness correction.

The two LFs look different (though the small number of stars does not allow to assess the statistical significance of this result), with the internal LF flatter than the external one as can be expected as a consequence of the equipartition of the energy. In a loosely populated cluster like Pal 1, dynamical evolution is very fast. The relaxation time is extremely short if we compare it with the typical values for GCs. In particular, Pal 1 has the shortest relaxation time in the compilation by Djorgovski (1993, D93), with a relaxation time at the half-mass radius $T_{rh} = 3.3 \times 10^7$ Gyr. Therefore, we do expect to detect mass segregation effects in its radial stellar distribution.

We calculated the MF corresponding to the LFs presented in Figure 9, using B94 models and the cluster parameters adopted in Section 4. The two annular MFs and the

global MF (i.e. the MF obtained for the entire cluster) are presented in Figure 10 (the global MF is shown shifted up by 0.2 units for clarity).

The best fitting power laws of the form $\xi = \xi_0 m^{-(1+x_{\text{MF}})}$ ($x_{\text{MF}} = 1.35$ for the Salpeter MF) are: $x_{\text{MF}} = -2.9 \pm 1.3$ for the inner MF, and $x_{\text{MF}} = -0.7 \pm 0.6$ for the outer one. The global MF (obtained from the global LF) has a slope $x_{\text{MF}} = -1.4 \pm 0.7$. As expected from the LFs, the MFs for the two annuli showed in Figure 10 are different (though this result is of low statistical significance), with the inner MF showing a reversed slope with respect to the outer one.

6. Dynamical analysis

In order to shed light on the real nature (open *vs.* globular) of Pal 1 we have also compared the structural parameters of Pal 1 with those of the globular and open cluster populations.

We derived the density profile of Pal 1, making radial star counts in equal-logarithmic steps, adopting the same selections in the CMD used to extract the LF. The result is shown in Figure 11 in which we show our star counts (closed circles), corrected for completeness and field object contamination. The open circles represent the light profile of Pal 1 published by Trager, et al, (1995, T95). Our star counts, transformed into magnitudes, have been shifted to match the T95 surface brightness profile.

One of the main problems in obtaining the profile of Pal 1 was to find its center. Choosing a wrong center in a loosely populated cluster with a small number of stars like Pal 1 would produce spurious trends in the central part of the profile (T95). We tried many algorithms like the ones listed in Picard & Johnston (1993), finding that the most reliable results could be obtained with the iterative centroiding algorithm by Aurière (1982).

The density profile clearly shows the presence of a flat core. Figure 11 shows no evidence for flattening of the T95 profile, probably consequence of incorrect centering of the star counts or an erroneous crowding correction in their starcounts (the most central point in T95 is from former star counts by King et al, 1968). The small number of cluster members has prevented us from extracting density profiles for stars of different mass: the density profile presented here is the profile for all the stars counted to the limit of the photometry (and corrected for completeness). Our data set allows a reliable estimate of the field object contamination, which is quite high (as already seen from the CMD of Figure 3). The background level was determined by counting stars outside $350''$ from the center of the cluster: *i.e.*, in the external field. The value used for the Pal 1 profile is $4.55 \text{ stars/arcmin}^2$, as shown in Figure 11.

We have fitted the radial profile with a single mass isotropic King (1966) model to extract the structural parameters of Pal 1. The best fitting model has a concentration parameter $c = 1.6$, a core radius of $r_c = 13.5''$ and a half-mass radius $r_h = 41''$, values that are well within the range observed for other Galactic GCs. The concentration parameter $c = 1.6$ is higher than the typical open cluster concentration parameters: none of the open clusters listed in Danilov & Seleznev (1994) has such a high c value. The central surface brightness is $\mu_V(0) = 20.93 \pm 0.25$, while the surface brightness at the half-mass radius is $\mu_V(r_h) = 23.52 \pm 0.25$. The tidal radius obtained from the model is $r_t = 525''$ even if beyond $\simeq 350''$ the star density of the model imply a total number of cluster stars less than one². This is due to the small total number of cluster stars: integrating the global LFs presented in Table 3, down to the adopted limit for our photometry ($V = 23.25$), we have a total number of $N_{tot} = 342 \pm 21$ stars. which correspond to a total integrated

²BS95 found a higher value for r_c and r_t (tidal radius), but without a direct measure of the background/foreground star contamination.

absolute magnitude $M_V = -2.54 \pm 0.50$. This value places Pal 1 at the lower end of the globular cluster luminosity function. Using the above estimate for the total absolute magnitude and the relation by Mandushev, Spassova, and Stanaeva (1991, eq. 4) we obtain $\log(m/m_\odot) = 3.1 \pm 0.3$ for the total cluster mass.

Even if the structural parameters of Pal 1 are very similar to the ones observed in other GCs, its global MF is different. As shown in Figure 12, the Pal 1 global MF slope falls completely outside the correlation between the mass function slope with the cluster Galactic position (R_{GC} , Z_{GP}), and metallicity [Fe/H] proposed by Djorgovski, Piotto, & Capaccioli (1993, DPC). This could be an evidence that the initial MF of Pal 1 was significantly different from the other 21 GCs shown in Figure 12. Another possibility is that, while the correlation by DPC holds for clusters with a mass function evolved by tidal shocks (Capaccioli, Piotto, & Stiavelli 1993), the MF of Pal 1 could be evolved as a consequence of another dynamical mechanism that can be tentatively identified as the stellar evaporation from the cluster. Indeed, in the recent work on the destruction rate of GCs by Gnedin & Ostriker (1996), Pal 1 has one of the highest evaporation destruction rates, while the values due to tidal shocks are comparable to the ones for other halo GCs (Gnedin & Ostriker 1996). Moreover, Johnstone (1993, J93) analyzing the evaporation escape rate of stars in GCs using multi-mass King models, found that the MF can be modified in a remarkable way. The effect is always toward a flattening of the MF and depends on the relaxation time: it is faster for very low concentration and/or loosely populated clusters. However, we cannot really say, without a simulation suited to Pal 1, if its observed MF is a consequence of evaporation only. Solving this problem would give us some information on the formation of this cluster. In the case of Pal 1, we can only calculate (following J93) the present evaporation destruction time, T_{ev} , assuming a constant rate of evaporation: $T_{ev} = 24 \times T_{rh} = 0.74$ Gyr: this shows that Pal 1 is very likely on the verge of destruction.

7. Summary and Discussion

The principal parameters of Pal 1 obtained in the present work are summarized in Table 4. The main results are:

- Pal 1 is very loosely populated: $N_{tot} = 342 \pm 21$ stars down to V mag 23.25, $M_V = -2.5 \pm 0.5$, and $M = 1300 \pm 600m_{\odot}$
- The mean features of the CMD are clearly defined for the internal region, though no obvious HB stars can be identified. Consequently, any cluster parameter based on the HB location must be considered very uncertain.
- In comparison to 47 Tucanae and M 71, Pal 1 seems to be younger than the typical galactic GCs.
- By comparison with isochrones, Pal 1 appears to have an age between 6.3 and 8 Gyr. Consequently, if we consider Pal 1 as a GC, it would be the youngest among the Milky Way GCs and the most metal rich halo GC. Alternatively, it would be one of the oldest open clusters.
- A surface density profile is presented and compared with previous data. Pal 1 does not show any evidence of core collapse: its central profile is flat. The best fitting single mass King model gives: $\mu_V(0) = 20.93$, $c = 1.6$ and $r_c = 13.5''$. If Pal 1 is an old open cluster, it is very peculiar, not only because of its position in the Galaxy ($R_{GC} = 17.3$ kpc, $Z_{GP} = 3.7$ kpc), but also for its concentration parameter ($c = 1.6$), which is higher than in any other open cluster.
- The observed luminosity function shows some evidence of mass segregation, as expected on the basis of the very short relaxation time of the cluster.

Consequently, also the MF slope varies with radius, though this result is statistically less significant.

- The global MF has a slope $x_{MF} = -1.4 \pm 0.7$. The Pal 1 MF slope does not follow the general trend with metallicity and Galactic position proposed by DPC: if this is an indication of evolution, the MF of Pal 1 has not been modified only by tidal shocks. In view of the short relaxation time, it might have been modified by evaporation. Another interesting possibility is that the initial MF of Pal 1 was quite different from that of other halo GCs.
- Evaporation implies a destruction time of $T_{ev} = 0.74$ Gyr: Pal 1 is very likely on the verge of destruction.

In conclusion, interpreted as an open cluster, Pal 1 would be very peculiar, at least in terms of position and morphology. On the other hand, we point out that there is a growing body of evidence for the existence of a small group of Galactic GCs that appear to be significantly younger than the average Galactic GC population. Pal 12 (Stetson et al, 1989; Gratton & Ortolani 1988) and Rup 106 (Buonanno et al, 1993; Da Costa, Armandroff, & Norris 1992) are 3-5 Gyrs younger than the bulk of GCs having similar metallicities. Arp 2 (Buonanno et al, 1995a), Terzan 7 (Buonanno et al, 1995b) and IC4499 (Ferraro et al, 1995) are other young candidates recently discovered. Pal 1 might be the youngest member of this group.

Many authors have tried to understand the existence of these young globular clusters: formation from clouds that have survived in the halo (Searle & Zinn 1978), inter-galactic clusters captured by the Milky Way (Lin & Richer 1992, Buonanno et al, 1995b), objects formed via interactions between the Galaxy and the Magellanic Clouds (Fusi Pecci et al, 1995) or other satellites which may have long since merged with our Galaxy (Majewski

1993, Lynden-Bell & Lynden-Bell 1995). Though other explanations are possible, the fact that the MF of Pal 1 seems to differ significantly from the MFs of 21 old GCs might be an interesting indication of a different origin for this object. This fact coupled with the young age might be a further evidence that Pal 1 is to be considered a member of a different globular cluster population, with a different formation process and time. It would be of great interest to compare the MF of this cluster with the MFs of other young candidates in order to check this hypothesis. Dynamical calculation of the evaporation effects are also needed, in order to correctly interpret the MF of Pal 1.

This project has been partially supported by the Agenzia Spaziale Italiana. The observation run has been supported by the European Commission through the Activity “Acces to Large-Scale Facilities” within the Programme “Training and Mobility of Researchers”, awarded to the Instituto de Astrofísica de Canarias to fund European Astronomers access to its Roque de Los Muchachos and Teide Observatories (European Northern Observatory), in the Canary Islands. We recognize partial support by the Instituto de Astrofísica de Canarias (grant P3/94) and by a Spanish-Italian integrated action. We thank Prof. Jack Sulentic for the careful reading of the manuscript.

REFERENCES

- Abell, G. O. 1955, *PASP*, 67, 258.
- Alcaino, G., & Liller, W. 1987, *ApJ*, 319, 304.
- Aparicio, A., & Gallart, C. 1995, *AJ*, 110, 2105.
- Armandroff, T. E., & Da Costa G.S 1986, *AJ*, 92, 777.
- Armandroff, T. E., & Da Costa G.S 1991, *AJ*, 101, 1329.
- Aurière, M. 1982, *A&A*, 109, 301.
- Bell, R., Vandenberg, D. A. 1987, *A&AS*, 63, 335.
- Bertelli, G., Bressan, A., Chiosi, C., Fagotto, F., & Nasi E. 1994, *A&AS*, 106, 275
- Borissova, J., & Spassova, N. 1995, *A&AS*, 110, 1
- Buonanno, R., Corsi, C. E., & Fusi Pecci, F. 1989, *A&A*, 216, 80
- Buonanno, R., Corsi, C. E., Fusi Pecci, F., Richer H. B., & Fahlman G. G. 1993, *AJ*, 105, 184
- Buonanno, R., Corsi, C. E., Fusi Pecci, F., Richer H. B., & Fahlman G. G. 1995a, *AJ*, 109, 650
- Buonanno, R., Corsi, C. E., Pulone, L., Fusi Pecci, F., Richer H. B., & Fahlman G. G. 1995b, *AJ*, 109, 663
- Burstein, D., & Heiles, C. 1982, *AJ*, 87, 1165
- Capaccioli, M., Piotto, G., & Stiavelli, M. 1993, *MNRAS*, 261, 819
- Da Costa, G. S., Armandroff, T. E., & Norris, J. E. 1992, *AJ*, 104, 154

- Danilov, V. M., & Seleznev, A. F. 1994, *Astron. and Astroph. Trans.*, 6, 85
- Dean, J. F., Warner, P. R., Cousins, A. W. J. 1978, *MNRAS*, 183, 569
- Djorgovski, G. 1993, in *Structure and Dynamics of Globular Clusters*, ed. by S. G. Djorgovski and G. Meylan (ASP, San Francisco), p. 373
- Djorgovski G., Piotto G., & Capaccioli M. 1993, *AJ*105, 2148
- Ferraro, I., Ferraro, F. R., Fusi Pecci, F., Corsi, C. E., & Buonanno, R. 1995, *MNRAS*, 275, 1057
- Friel, E. D. 1995, *ARA&A*, 33, 381
- Fusi Pecci, F., Bellazzini, M., Cacciari, C., & Ferraro, F. R. 1995, *AJ*, 110, 1664
- Gnedin, O. Y., & Ostriker, J. P. 1996, *ApJ*, in publication
- Gratton, R. G., & Ortolani, S. 1988, *A&AS*, 73, 137
- Grundahl, F., 1996, *ASP Conf. Ser.*, Vol 92, 273
- Hesser, J.E., Harris, W.E., Vandenberg, D.A., Allwright, J.W.B., Shott, P., & Stetson, P.B. 1987, *PASP*, 99, 739 (H87)
- Hodder, P., Nemec, J., Richer H., & Fahlman G., 1992, *AJ*, 103, 460
- Johnstone, D. 1993, *AJ*, 105, 155
- Kaluzny J., 1994, *A&AS*, 108, 151
- Kaluzny J., Wysocka A., Krzeminski W., 1997 (In preparation)
- King, I. R., 1966, *AJ*, 71, 64
- King, I. R., Hedeman, E., Hodge, S., & White, R. 1968, *AJ*, 73, 456

- Kinman, T. D., Rosino, L. 1962, *PASP*, 74, 499
- Landolt, A. 1992, *AJ*, 104, 340
- Lin, D. N. C., & Richer, H. B. 1992, *ApJ*, 388, 57
- Lynden-Bell, D., & Lynden-Bell, R. M. 1995, *MNRAS*, 275, 429
- Majewski, S. R. 1993, *ARA&A*, 31, 575
- Mandushez, G., Spassova, N. & Staneva, A., 1991, *A&A*, 252, 94
- Ortolani, S., & Rosino, L. 1985, *Mem.S.A.It.*, 56, 105
- Picard, A., & Johnston, P. 1993, *A&A*, 276, 331
- Piotto, G., King, I. R., Capaccioli, M., Ortolani, S., & Djorgovski, G. S. 1990, *ApJ*, 350, 662
- Reid M.J., 1993, *ARA&A*, 31, 345
- Richer, H., & Fahlman, G., 1988, *ApJ*, 325, 218
- Rosenberg A., Piotto G., Saviane I., Aparicio A. & Gratton R., 1997, *ApJL* (Submitted)
- Searle, L., & Zinn, R., 1978, *ApJ*, 225, 357
- Stetson, P. B., 1987, *PASP*, 99, 191
- Stetson, P. B., Hesser J. E., Smith, G. H., Vandenberg, & D. A. Bolte, M. 1989, *AJ*96, 909
- Trager, S. C., King, I. R., & Djorgovski, G. S., 1995, *AJ*, 109, 218
- Vandenberg, D. A., Bolte, M., & Stetson, P. B. 1990, *AJ*, 100, 445
- Webbink, R. 1985, *IAU Symp. Dynamics of Stars Clusters*, eds. J. Godman and P. Hut, p. 541

Fig. 1.— Central 4.3×4.3 arcmin image of Pal 1, taken with the I filter and an exposure time of 600 s.

Fig. 2.— The aperture photometry correction as a function of the FWHM for all the observed standard stars. The dotted line represents a linear fit to the data.

Fig. 3.— Color-magnitude diagrams for three Pal 1 regions and for the external field.

Fig. 4.— Fiducial points for Pal 1 plotted over the CMD for the central $80''$. The error bars represent the 1σ width of the MS.

Fig. 5.— Color-magnitude diagram for the central $80''$: each box contains the expected number of field stars within the sketched color and magnitude limits.

Fig. 6.— Determination of the Pal 1 distance modulus from the comparison of its fiducial line with the fiducial lines of 47 Tuc. The fiducial line of M71 is also shown. (See text for details).

Fig. 7.— The Pal 1 fiducial points and a set of isochrones from Bertelli et al, (1994) has been registered so that the TOs coincide. The metallicity of the isochrones is $Z = 0.004$ and the ages are, from left to right, 16, 12.5, 10, 8 and 6.3 Gyrs; this comparison shows that the shapes of the Pal 1 CMD is compatible with an age in the interval 6.3 to 8 Gyrs.

Fig. 8.— A subset of isochrones from Bertelli et al, (1994) overplotted on the Pal 1 CMD; the diagram was corrected for the assumed distance modulus and reddening (see text), and the isochrones were shifted by 0.03 mag blueward to match the observed MS. An age of 8 Gyr is the one that better reproduces the data.

Fig. 9.— Observed luminosity functions for the cluster center ($r < 30''$), the outer part ($30'' < r < 270''$), and for the background field outside $r > 350''$ from the center. The cluster LFs were corrected for completeness and field contamination; the outer LF was normalized to the inner one using the first two bins (i.e. shifted up by 1.853 units).

Fig. 10.— Mass functions of Pal 1 obtained from the LFs of Figure 9 using B94 models for $[Fe/H] = -0.7$ and age=8.0 Gyr.

Fig. 11.— Close dots represents the radial star counts coming from the present photometry of Pal 1. Open circles are the data from Trager et al, (1995), while the solid line represents the best fitting isotropic single mass King model. See text for a detailed explanation.

Fig. 12.— Trivariate relation between the position (R_{GC}, Z_{GP}), metallicity $[Fe/H]$ and the slope of the global mass functions for 21 old GCs of our Galaxy (close dots). The star represents the position of Pal 1.

TABLE 1. Observing Log

Central Field				
Date	f.	t_{exp}	airm.	FWHM
08/11/94	V	60	1.612	1"1
08/11/94	V	800	1.617	1"1
08/11/94	V	800	1.630	1"2
08/11/94	V	800	1.645	1"2
08/11/94	V	800	1.664	1"2
08/11/94	V	800	1.683	1"3
08/11/94	V	800	1.704	1"2
10/11/94	V	1200	1.601	1"2
10/11/94	V	1200	1.590	1"2
08/11/94	I	30	1.728	1"0
08/11/94	I	400	1.735	1"1
08/11/94	I	400	1.749	1"2
08/11/94	I	400	1.765	1"2
08/11/94	I	400	1.783	1"2
08/11/94	I	400	1.801	1"2
10/11/94	I	600	1.609	1"2
10/11/94	I	600	1.585	1"1
External Field.				
Date	f.	t_{exp}	airm.	FWHM
09/11/94	V	60	1.696	1"0
09/11/94	V	4×1200	1.598	1"2
10/11/94	V	1200	1.580	1"2
09/11/94	I	30	1.580	1"0
09/11/94	I	4×600	1.656	1"2
10/11/94	I	60	1.580	1"0